Electronic Supplementary Material (ESI) for Biomaterials Science.
This journal is © The Royal Society of Chemistry 2024

Supplementary Information

Design, clinical applications and post-surgical assessment of bioresorbable 3D-printed craniofacial composite implants

Sara Targońska[1,2+], Monika Dobrzyńska-Mizera[3+], Maria Laura Di Lorenzo[4*], Monika Knitter[3], Alessandra Longo[4,5], Maciej Dobrzyński[6], Monika Rutkowska[7], Szczepan Barnaś[7], Bogdan Czapiga[7], Maciej Stagraczyński[7], Michał Mikulski[8], Małgorzata Muzalewska[9+], Marek Wyleżoł[9+], Justyna Rewak – Soroczyńska[1], Nicole Nowak[1], Jacek Andrzejewski[3], John M. Reeks[1] and Rafal J. Wiglusz[1,10*]

[1]Institute of Low Temperature and Structure Research, PAS, Okolna 2, PL-50-422 Wroclaw, Poland

[2]Department of Molecular Sciences, Swedish University of Agricultural Sciences, Box 7015, 75007 Uppsala, Sweden

[3]Institute of Materials Technology, Polymer Division, Poznan University of Technology, Piotrowo 3, 61-138 Poznan, Poland

[4]National Research Council (CNR), Institute of Polymers, Composites and Biomaterials (IPCB), Via Campi Flegrei, 34, 80078 Pozzuoli (NA), Italy

[5]National Research Council (CNR), Institute of Polymers, Composites and Biomaterials (IPCB), Via Paolo Gaifami 18, 95126, Catania (CT), Italy

[6] Department of Pediatric Dentistry and Preclinical Dentistry, Wroclaw Medical University, Krakowska 26, 50-425 Wroclaw, Poland

[7]4th Military Teaching Hospital, R. Weigla, Pl-50-981 Wroclaw, Poland

[8]NZOZ Artdent, Piekarska 11-13, 62-800 Kalisz, Poland

[9]Department of Fundamentals of Machinery Design, Faculty of Mechanical Engineering Silesian University of Technology, Gliwice, Poland

[10] Department of Organic Chemistry, Bioorganic Chemistry and Biotechnology, Silesian University of Technology, Krzywoustego 4, 44-100 Gliwice, Poland

E-mail: marialaura.dilorenzo@ipcb.cnr.it; r.wiglusz@intibs.pl; rafal.wiglusz@polsl.pl

S1.1. Modelling of the frontal lobe implant (*Medical Case no. 1*)

Within the first step of the modelling procedure, bone structures were recreated using the patient's skull computed tomography (CT) images. DICOM images generated from CT were then imported into specialized medical software to design a 3D model of the defective frontal bone. The process began with the initial segmentation and marking of working areas within three-planed 2D images. Then, the contours of the bone tissues were carefully marked, the working area was limited, and finally, a frontal bone 3D model was generated and saved as a mesh model.

The second step of the modelling procedure includes designing an implant shape based on a 3D model of the defective frontal lobe, as described above. The anatomical model constituted the boundary conditions for creating a fitted implant. Using selected software tools from the Geomagic Freeform Plus 2021 system, a scaffold model was created that precisely matched the patient's bone loss (see Figure 2b and Figure S1b). The implant was equipped with holed tabs to enable fixation with titanium screws. In addition to modelling, the Freeform Plus system can perform diagnostic and geometrical form verification of the virtual model. This includes thickness maps, curvature change maps, measuring distances between indicated model features, etc. In this case, it is critical that the implant thickness match the thickness of the skull in the fixation area and that its edges perfectly match the defect shape.

A standard procedure finishes at this point. However, this patient required reoperation due to the leakage of cerebrospinal fluid. As a result, the authors took the opportunity to improve the second implant's shape. The leakage pressure deformed implant curvature, especially in the fixation area. Therefore, another fixation method, including titanium plates and screws, was proposed. Virtual model of the new implant was designed according to the procedure described above. The scaffold's shape was improved such that its outer curvature would fit that of the skull. Furthermore, holed tabs were replaced with a smooth finish (see Figure 2c and Figure S1c,e). Moreover, as recommended by the surgeon, the edge of the implant

was shaved down so the *Cranioimplant* could be placed loosely in the hole, while the thickness of the central part of the implant was reduced to 4 mm.

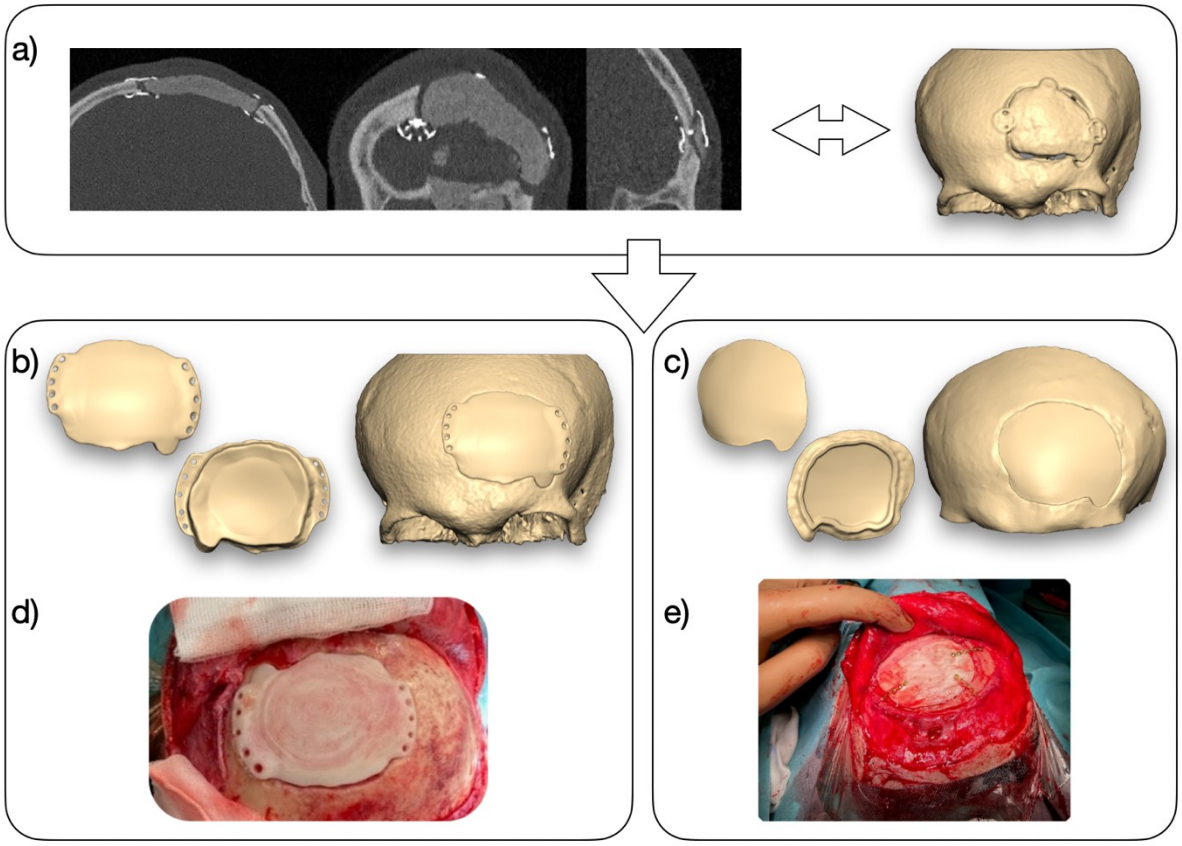

Figure S1. Medical case no.1 a) view of the skull loss filled with a medical cement and Craniofix system, b) the first implant model, also located in the bone defect, c) the second implant model located in the bone defect, d) and e) the first and second 3D-printed graft placed in the frontal lobe.

S1.2. Modelling of the mandibular implant (*Medical Case no. 2*)

The mandibular bone-implant was designed for the reconstruction of the patient's craniofacial after a car accident. The patient had undergone a fractured mandible fusion procedure with the use of reconstructive titanium plates. The procedure allowed the bone to heal, but no support for tooth reconstruction was created. As a result, an additional craniofacial reconstruction, the mandibular bone restoration, was proposed. Grafting of the bone loss with a personalised and resorbable *Cranioimplant* can likely aid in rebuilding an appropriate jaw arch.

The DICOM images created from CT scans were used to recreate the actual skeletal system (see Figure 2d and Figure S3a). On this basis, a virtual model of the lower jaw, together with fixation elements, was obtained. After consultations with the main surgeon, it was decided that two variants of the model should be prepared. The first operation scenario assumed a situation where the lower plate could not be removed. In such a case, the implant would only cover the upper part of the mandible to match the existing plate (Figure 2e v.1 and Figure S2b). The second option anticipated removing both mounting plates and replacing them with one implant (Figure 2e v.2 and Figure S2c).

The first implant model covered the entire height of the mandibular bone and overlapped its posterior section from the top to bottom. This arrangement provided a large contact area which is conducive to osteogenic stimulation as well as improved *Cranioimplant* fixation. The second model was precisely fitted to the existing reconstructed lower plate and only overlapped the top mandibular bone (with extended sides for better fixation). The second model was recommended due to its more advantageous mechanical properties and potential for bone reconstruction.

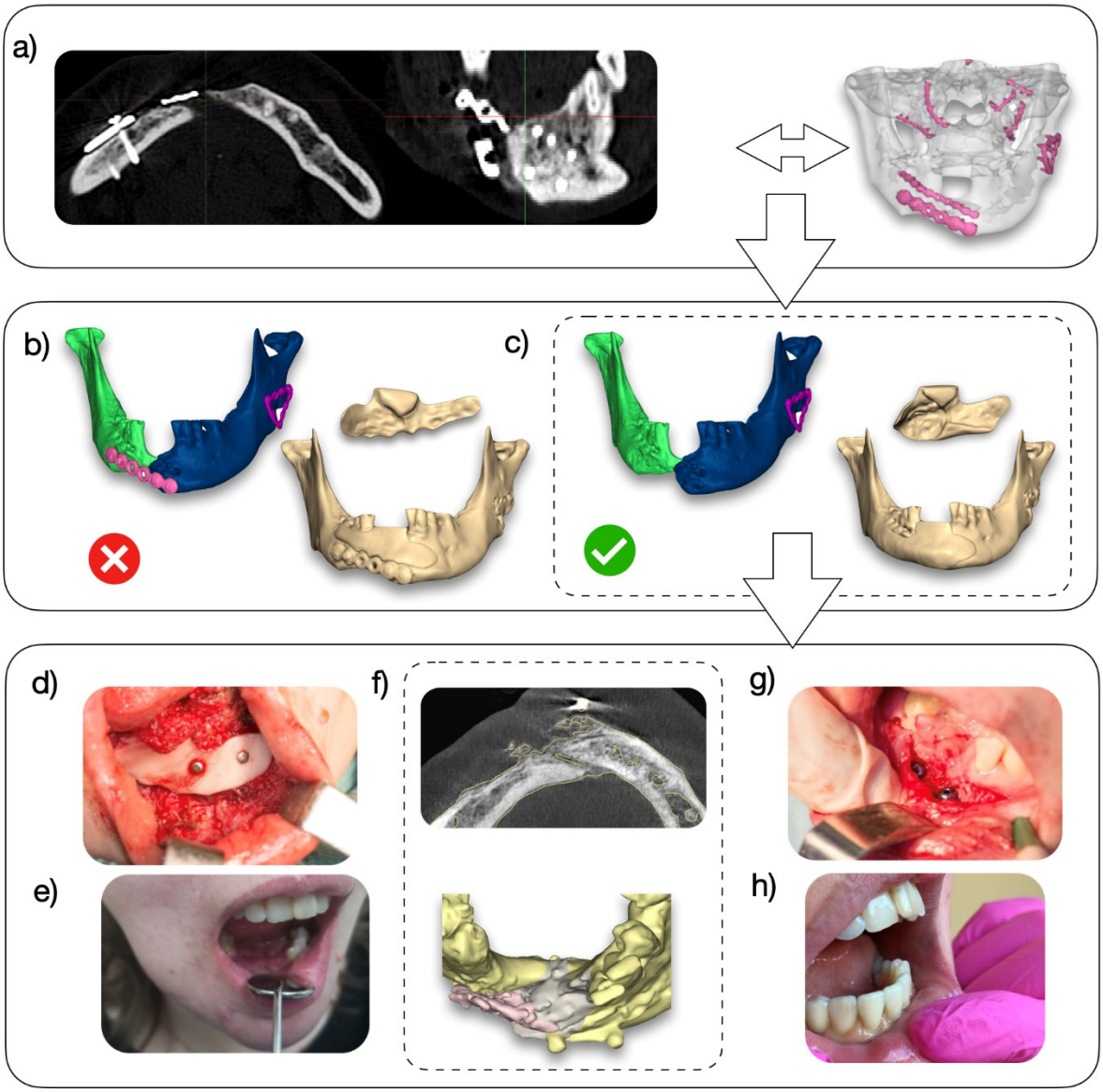

Figure S2. a) CT scan of the patient's jaw (with artefacts) and a 3D model of the mandible before the procedure, b) discarded implant model, c) recommended implant model, d) view of the patient during the operation, e) view of the patient during the follow-up visit, f) remodeling of bone tissue, g) view of the patient after grafting of the dental grafts, h) prosthetic restoration.

S1.3. Modelling of the cleft palate implant (*Medical Case no. 3*)

As previously described, based on the CT results and following DICOM images, a model of the patient jawbone was prepared. Then, the models of defective areas were selected and saved as mesh models.

Subsequently, the cleft palate implant was modelled (Figures 2h and S3b-c). Fixation of the 3D-printed implant was based on a tightly fitted shape, ensuring a clear positioning in the recipient's defect. Wherefore, only one way of introducing the scaffold was possible which ensured shortening of the surgery. Additionally, stabilising arms covering the adjacent bone were designed (Figures 2h and S3b-c).

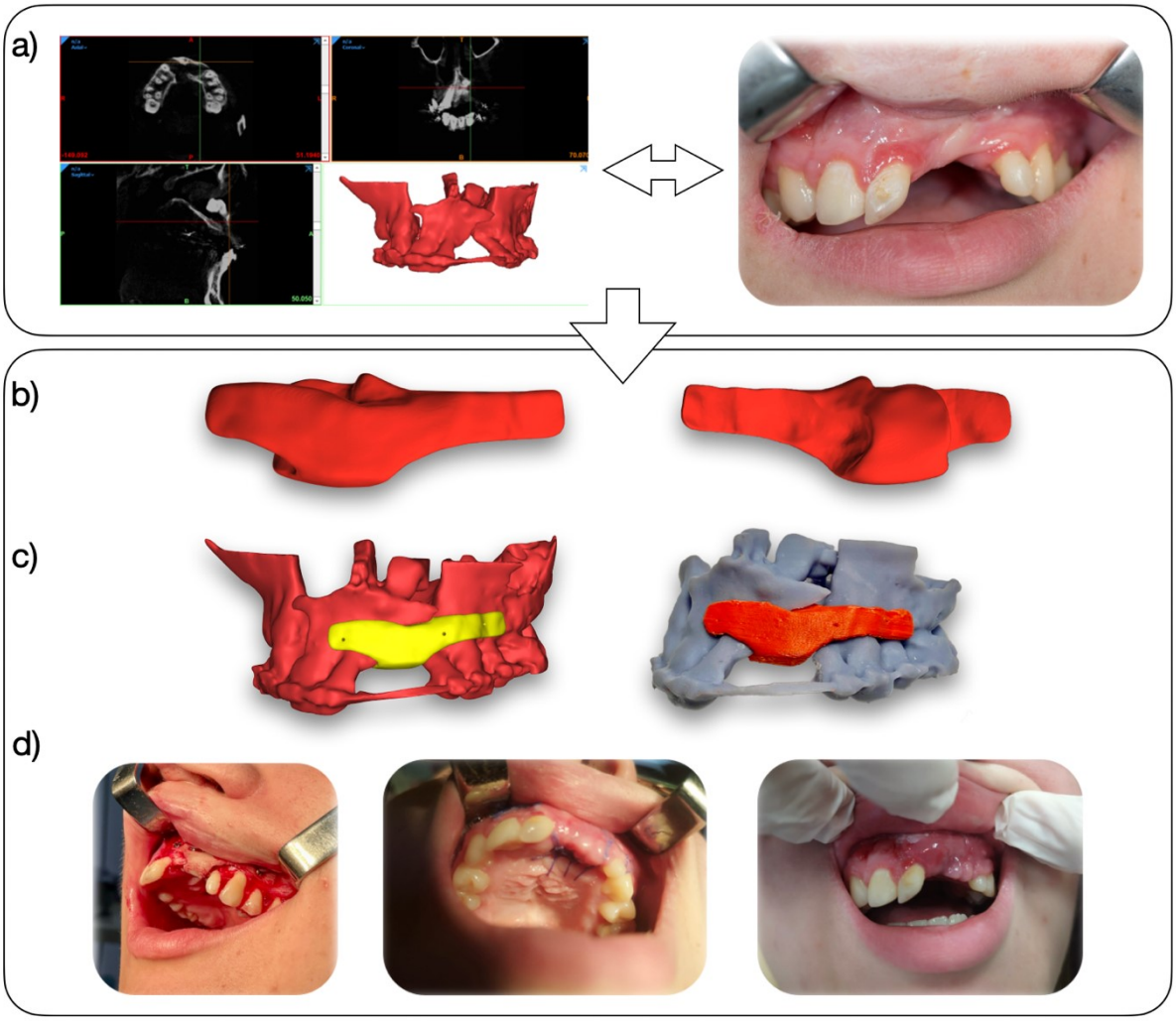

Figure S3. a) CT scan, jaw 3D model, and view of the patient's condition before the surgery, b) front and back view of the implant, c) view of the implant model and its 3D-printed prototype in the graftation place, d) view of the patient during surgery and at follow-up visits.

S1.4. The implant geometrical accuracy

The implants' geometrical precision is crucial and determines successful utilization of the personalized technologies [1-4]. Therefore, an optical scanner measurements were involved to confirm sufficient reproduction level of the CAD designed 3D models. The C*ranioimplant* planned for reconstruction of the frontal lobe defect (Figure 2b) was selected for in-depth geometrical analysis due to its relatively large size, which may lead to substantial deformations. Additionally, in this particular case it was crucial that fixation holed tabs preserved their shape and curvature as large deviations in these areas might have resulted in improper positioning of the implant during surgery.

Methodology

The dimensional accuracy measurements of the *Cranioimplant* model were performed using an optical scanner. A GOM (Zeiss) Triple Scan scanner, a structured light method, and an accuracy of 0.03 mm were used. Prior to measurement, the part surface was covered with a thin layer of antireflecting coating. The results of the scanning procedure were collected as triangular mesh and exported in STL (Standard Tessellation Language) format file for analysis in GOM Inspect software.

Results

The optical scanner measurement results, with the obtained implant mesh, mesh/CAD model comparison and geometry deviations, are presented in Figure S4. The mesh model was reproduced with visible individual layers created upon the production process. The mesh/CAD model comparison is created upon the fit alignment analysis between the actual model obtained in the measurements and the geometry used to generate the 3D printer's machine code. The deviation values, also represented by color palette on a ± 0.5 mm scale, was plotted on the mesh model.

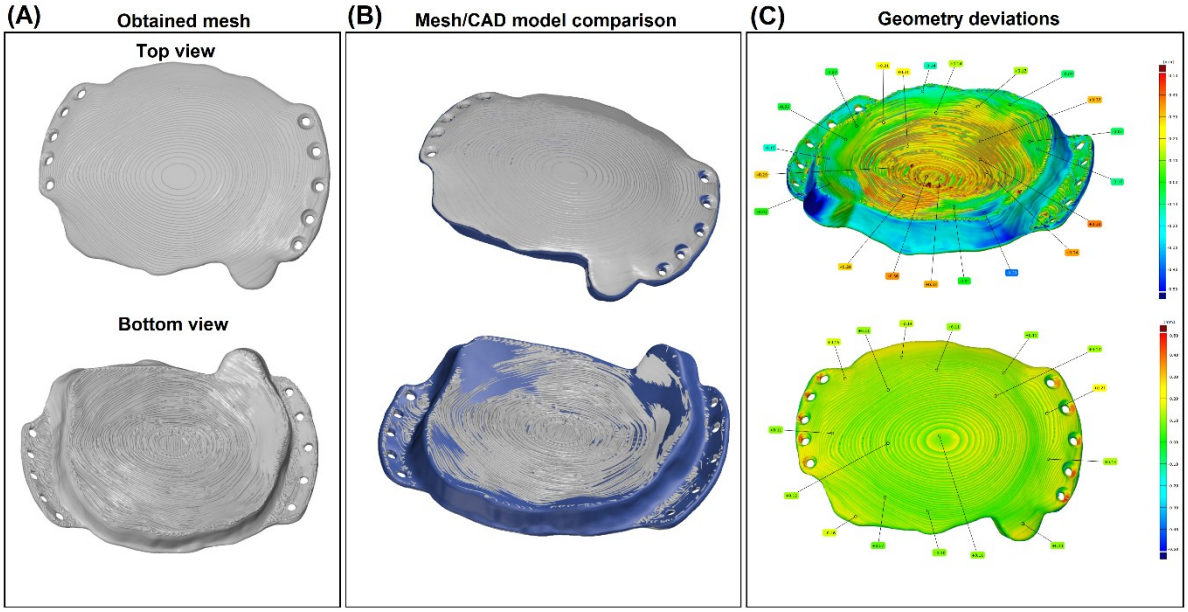

Figure S4. The optical scanning measurements: mesh model obtained during scanning (a), mesh/CAD model comparison (b), geometry deviations analysis (c).

The analysis indicated a high level of the CAD model reproduction as the deviation values rarely exceed 0.5 mm, proving the implant usability for the bone reconstruction procedures. The outcomes also confirmed that the positioning of the model during printing was correct. Slight negative deviations (blue), visible around the implant periphery, occurred due to material shrinkage. Deviations of less than 0.5 mm in the area ensure a proper fit between the implant and the patient's native bone and ease fixation during the surgery. Contrarily, the highest positive deviations occurred within the bottom Cranioimplant part, as expected, as this area is equipped with support structures known for filament accumulation. Therefore, the support structures were positioned in places with the lowest requirements for dimensional accuracy, i.e. areas without contact with bone tissue. Moreover, the holed tabs' accuracy was analysed, proving only minor shape deviations were recorded in the region. Interestingly, positive deviations near the outer implant edges appeared, related to the circumferential shrinkage, not affecting the overall mapping of the holes' positioning.

Literature:

1. K. Moiduddin, S. H. Mian, U. Umer, H. Alkhalefah, F. Ahmed and F. H. Hashmi, *Polymers (Basel)*, 2023, **15**, 886.
2. E. George, P. Liacouras, F. J. Rybicki and D. Mitsouras, *RadioGraphics*, 2017, **37**, 1424–1450.
3. M. Yeung, A. Abdulmajeed, C. K. Carrico, G. R. Deeb and S. Bencharit, *J Prosthet Dent*, 2020, **123**, 821–828.
4. M. Robles-Medina, M. Romeo-Rubio, M. P. Salido and G. Pradíes, *Curr Oral Health Rep*, 2020, **7**, 361–375.